Seal bomb explosion sound source characterization

Sean M. Wiggins ; Anna Krumpel; LeRoy M. Dorman; John A. Hildebrand; Simone Baumann-Pickering

Check for updates

CrossMark

View Online   Export Citation

JASA ARTICLE

Seal bomb explosion sound source characterization

Sean M. Wiggins,[1,a)] Anna Krumpel,[2] LeRoy M. Dorman,[1] John A. Hildebrand,[1] and Simone Baumann-Pickering[1,b)]

[1]*Scripps Institution of Oceanography, 9500 Gilman Drive, La Jolla, California 92093-0205, USA*
[2]*Eberhard Karls University of Tuebingen, Auf der Morgenstelle 28, 72076 Tuebingen, Germany*

ABSTRACT:

Small explosive charges, called seal bombs, used by commercial fisheries to deter marine mammals from depredation and accidental bycatch during fishing operations, produce high level sounds that may negatively impact nearby animals. Seal bombs were exploded underwater and recorded at various ranges with a calibrated hydrophone to characterize the pulse waveforms and to provide appropriate propagation loss models for source level (SL) estimates. Waveform refraction became important at about 1500 m slant range with approximately spherical spreading losses observed at shorter ranges. The SL for seal bombs was estimated to be 233 dB re 1 μPa m; however, for impulses such as explosions, better metrics integrate over the pulse duration, accounting for the total energy in the pulse, including source pressure impulse, estimated as 193 Pa m s, and sound exposure source level, estimated as 197 dB re 1 μPa^2 m^2 s over a 2 ms window. Accounting for the whole 100 ms waveform, including the bubble pulses and sea surface reflections, sound exposure source level was 203 dB re 1 μPa^2 m^2 s. Furthermore, integrating the energy over an entire event period of multiple explosions (i.e., cumulative sound exposure level) should be considered when evaluating impact.

I. INTRODUCTION

Seal bombs, also known as explosive pest control devices and seal deterrent devices, among other names, are hand-thrown pyrotechnic devices capable of exploding underwater and are used as a means to deter marine mammals during commercial fishing operations. For example, seal bombs were used at least as early as 1980 in the eastern tropical Pacific (ETP) yellow fin tuna purse-seine fishery to control dolphin swimming direction during all stages of net setting (Cassano *et al.*, 1990). More recently, underwater recordings of thousands of explosions per month were spatially and temporally correlated with commercial landings data of California market squid, suggesting that seal bombs were used extensively during squid fishing operations (Meyer-Löbbecke *et al.*, 2016).

A primary concern with the use of seal bombs is potential harm to marine mammals, especially animals in close proximity to the explosions. While non-hearing physical damage was estimated for close ranges (<4 m; Myrick *et al.*, 1990a), hearing related impacts such as temporary threshold shift (TTS) and permanent threshold shift (PTS) or loss of hearing may occur at more distant ranges (e.g., Finneran, 2015). Furthermore, behavioral responses to explosions of the targeted animals, in addition to non-targeted marine

mammals, may cause harm by altering biologically significant behaviors such as foraging (e.g., Southall *et al.*, 2007).

Seal bomb source characterization is needed to provide metrics for managing marine noise pollution and mitigating effects on marine mammals due to high sound pressures from these explosions. We describe an experiment offshore of Southern California in which seal bombs were deployed and exploded at various ranges from an underwater sound recorder. The received sound pressure waveforms were analyzed, and various metrics were estimated to provide a characterization of the seal bomb source, including source level (SL), an important metric for marine noise management.

II. METHODS

A. Experiment overview

Experimental operations were conducted in late spring 2017, offshore of Southern California, when more than 600 seal bombs were individually exploded underwater over three days and recorded with an autonomous hydrophone. The free-floating autonomous hydrophone recorded these explosions at various ranges from less than 300 m to more than 8 km while deployed a few hundred meters beneath the sea surface above seafloor depths ranging from 635 to 870 m (Fig. 1 and Table I). Global positioning system (GPS) receivers were attached to both the seal bomb deployment ship, Scripps Institution of Oceanography Research Vessel (R/V) Saikhon, and a sea surface float above the hydrophone

a)Electronic mail: swiggins@ucsd.edu, ORCID: 0000-0002-9686-035X.
b)ORCID: 0000-0002-3428-3577.

TABLE I. Autonomous acoustic recorder nominal locations for three deployments.

Deployment number	Date	Latitude (N)	Longitude (W)	Hydrophone depth (m)	Seafloor depth (m)
01	30 May 2017	32° 52.034′	117° 29.235′	265	715
02	01 Jun 2017	32° 52.052′	117° 27.750′	265	635
03	02 Jun 2017	32° 51.443′	117° 32.802′	265	870

to provide source-receiver ranges. These ranges along with measured sound pressures at the hydrophone receiver provided the measurements needed to estimate seal bomb source levels.

B. Seal bombs

Seal bombs are similar to pyrotechnic firework salutes that generate a loud report (i.e., bang) along with a bright flash when their explosive material, flash powder, is ignited. Flash powder is a low explosive that deflagrates (i.e., burns and builds up and then decreases pressure over the time of the explosion), although at a much faster rate than black powder (gunpowder), and should not be confused with detonation of high explosives, such as trinitrotoluene (TNT), where a shock wave (i.e., a wave front traveling faster than the speed of sound) is generated and maximum pressure is sudden but decays quickly and exponentially.

While there are different seal bomb manufacturers around the world using various amounts (~2–6 g) and different formulations of flash powder (Myrick *et al.*, 1990b), this study was limited to one type of seal bomb, the Seal Cracker Device, manufactured by Stoneco Energetics Systems LLC (Prescott Valley, AZ). The Seal Cracker

Devices, from here onward referred to as seal bombs, were ~8.3 cm long × 1.7 cm diameter cardboard tubes wrapped with yellow paper and a bright orange label with a ~6.7 cm long × 0.3 cm diameter green fuse protruding from one of the plastic-plugged ends [Fig. 2(a)]. Inside the tube were two chambers: a lower one with silica sand used to provide weight so that the seal bomb will sink upon deployment and an upper one containing flash powder and the unlit end of the fuse for deflagration initiation [Fig. 2(b)]. The seal bomb had a visco fuse that had a black powder core and was coated with nitrocellulose for water resistance so that it would continue to burn after deployment underwater. The fuse burn duration before explosion was about 8 s. Explosion depths were estimated to be 1–4 m (Myrick *et al.*, 1990b).

The seal bombs used in this study had a charge mass of 2.33 g of flash powder and used a standard formulation of about 64.0% potassium perchlorate ($KClO_4$) as the oxidizer and a fuel of 25% aluminum powder and 10% sulfur (Stonebraker, 2018). This charge mass was similar to common M-80 salutes classified as consumer fireworks.

During the experiment, the free end of the seal bomb fuse was ignited using a standard home-improvement-style push-button torch hose kit connected to a 400 ml (14 fluid oz) bottle of propane. After ignition, the seal bomb was tossed by hand into the water 5–10 m starboard and off the rear quarter of the R/V Saikhon while under way at ~3 m s^{-1}
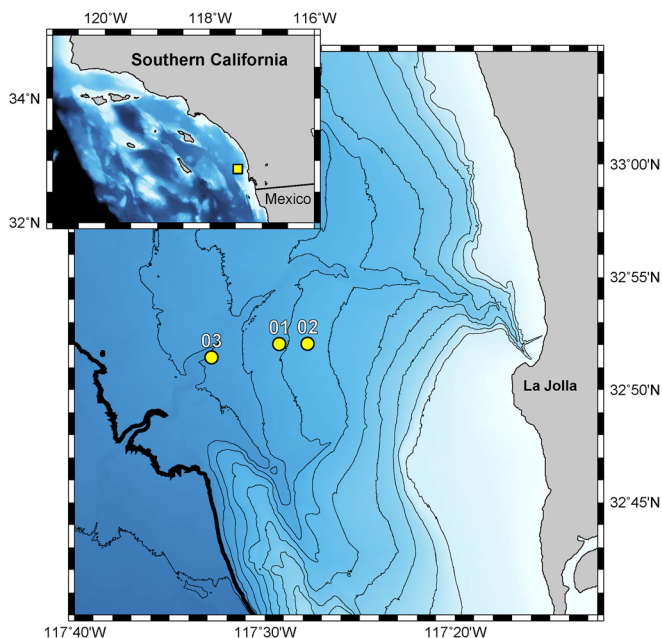
FIG. 1. (Color online) Bathymetric map of experiment area offshore of La Jolla, CA. The inset map yellow square shows the study area. Yellow circles 01, 02, and 03 were autonomous hydrophone deployment sites for 30 May and 1 and 2 June 2017, respectively. Thick contour was 1000 m depth, with thin contours at 100 m increments. Dark colors were deeper and farther offshore.
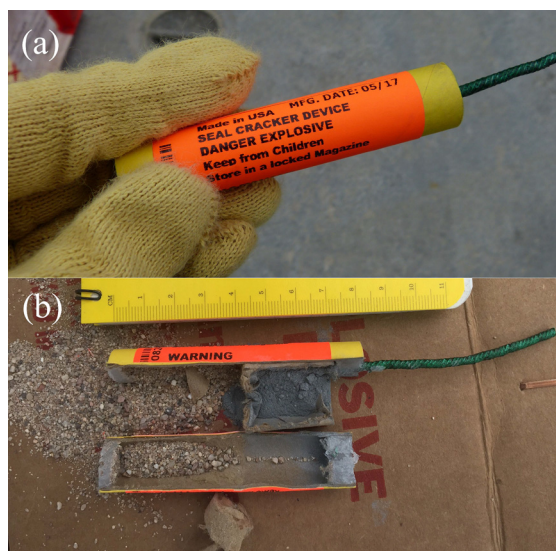

FIG. 2. (Color online) Seal bomb—Stoneco Energetics System, LLC Seal Cracker Device. (a) Seal bomb prior to ignition and deployment. (b) Seal bomb cut long-axis showing internal contents with two chambers: silica sand for sinking weight and gray flash powder with green fuse for underwater explosion.

(11 km h^{-1}; 6 kn). Seal bombs were deployed approximately every 30 s along a transit line, marked with the ship's GPS. Notes were logged for each seal bomb deployment including time, location, and type of explosion (good, dud, shallow) along with changes in deployment schedule due to deviations in ship track or pauses during marine mammal, fish, or bird presence to avoid their use in the proximity of marine animals.

C. Underwater recordings

To measure sound pressures of seal bomb explosions, recordings were made using an autonomous high-frequency acoustic recording package (HARP; Wiggins and Hildebrand, 2007). The HARP was configured to record at a 200 kHz sample rate with 16-bit samples onto laptop computer type hard disk drives. Since seal bombs generate high sound pressures and some source-receiver ranges were relatively short, the sensitivity of the hydrophone was reduced from standard HARP hydrophones by about 40 dB to prevent signal clipping. The hydrophone was constructed of two sensors: Benthos (North Falmouth, MA) AQ-1 for frequencies below 10 kHz and International Transducer Corporation (Santa Barbara, CA) 1042 for frequencies above. The sensors are specified as having approximately the same sensitivity of −201 dB re 1 V/μPa. The hydrophone signal conditioning electronics gain was set to be 10 dB with a full system peak clip level ∼200 dB re 1 μPa, and the full band frequency response (10 Hz–100 kHz) was calibrated in our lab at Scripps Institution of Oceanography so that absolute received sound pressures could be measured.

Typically, HARPs are deployed on the seafloor as bottom-mounted instruments or in a mooring configuration including an acoustic release system used for jettisoning ballast weight and instrument retrieval. For this study, the data logger housing and hydrophone were suspended beneath the sea surface in a multiple float and weight system such that the hydrophone was decoupled from vibrations and motions of the sea surface float (Fig. 3). The hydrophone was placed at 265 m depth, well below the thermocline to avoid problems with acoustic raypath refraction. Attached to a flagpole on the sea surface float about 1.5 m above the waterline in a plastic bag was a dog collar GPS [Garmin (Schaffhausen, Switzerland) Astro 32 with T5]. The dog collar transmitted positions every 2 min via radio frequencies to its receiver onboard the R/V Saikhon for logging. Float drift rate was less than 0.06 m s^{-1} (2 km h^{-1}; 0.1 kn). The receiver for the dog collar GPS also was used to record the ship GPS positions.

After recovery of the recorder, the hard disk drives were removed, and disk image files of raw data disks were generated for archiving and processing. Processing raw data into working data included uncompressing and creating multiple 37.5-min audio (wav format) files with high precision time stamps. The audio files were used to make long spectrograms to provide a graphical index for the data, allowing quick and easy access to sound events of interest
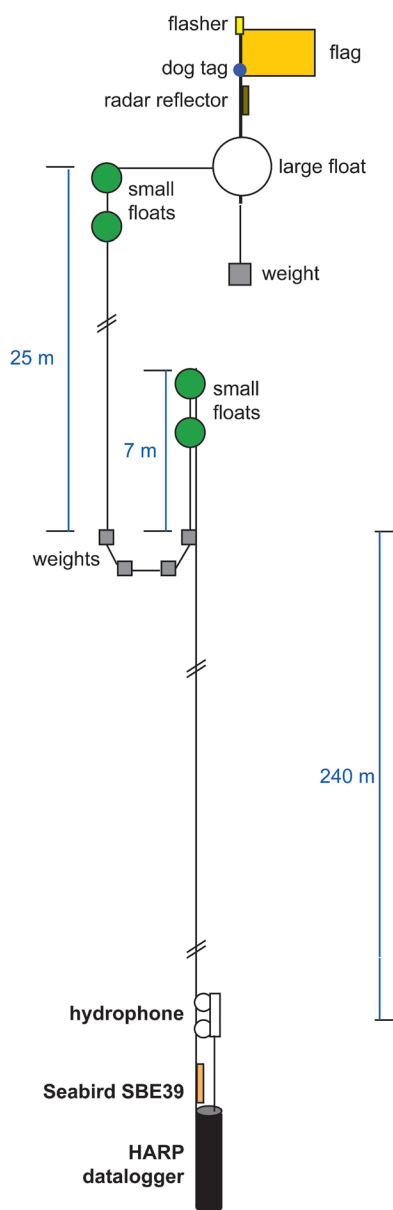

FIG. 3. (Color online) Autonomous acoustic recorder mooring configuration. The large white float was at the sea surface and included a flag, flasher, and radar reflector to prevent being struck by nearby transiting vessels. Also, attached to the flag was a dog collar GPS receiver, which transmitted locations back to R/V Saikhon. Beneath the sea surface on the mooring line was a system of floats and weights to decouple the sea surface motion from the hydrophone at 265 m depth. Hydrophone depth was confirmed via Seabird temperature-pressure logger.

(see the acoustic analysis software package, *Triton*; Wiggins and Hildebrand, 2007).

Software was developed in MATLAB (Mathworks, Inc., Natick, MA), to filter, automatically detect, measure amplitudes, and save snippets of received seal bomb shots from the audio files. An eighth order Chebyshev type 2 low-pass filter (LPF) with a stop band edge at 10 kHz was used on the waveforms to reduce apparent high-frequency transient effects from the hydrophone. We did not anticipate any effect from the filter on sound pressure estimates as most of the energy for shallow depth explosions is below 1 kHz with

J. Acoust. Soc. Am. **150** (3), September 2021

Wiggins *et al.* 1823

the source spectrum falling off rapidly to at least 20 dB lower around 10 kHz (Weston, 1960). The detector was a simple energy detector with the 0-peak sound pressure threshold set to ∼16 Pa (i.e., peak sound pressure level threshold = 144 dB re 1 μPa) to identify pulse first-arrival times. Snippet waveforms from 0.1 s before detection to 1.0 s after detection were saved as binary files. Additional software was developed to evaluate seal bomb shots, including metric calculations and plots.

D. Impulse metrics

Different metrics are used to describe different types of sound pressure signals, expressed in Pa. For example, continuous pressure wave signals from sources such as ships and sonar pings are typically reported as root mean square (rms) of the sound pressure, $p(t)$, over a time window, T,

$$p_{rms} = \sqrt{\frac{1}{T}\int_0^T p^2(t)dt},$$ (1)

where the time window is typically defined as the signal width 3 dB down from the peak sound pressure, the signal width 10 dB down from the peak sound pressure, or from 5% to 95% of the signal's total energy, described as −3 dB, −10 dB, and 90% rms, respectively. Impulsive sounds are usually not well-represented as rms because rms depends on the analysis window duration, which for transient signals is critical (e.g., Madsen, 2005). For example, the rms for a smoothly varying impulse, such as a Gaussian function or underwater explosion, is typically lower for 90% rms than for −3 dB rms because of a longer time window for the 90% rms metric.

Impulsive or transient sounds, such as those from seismic air guns or underwater explosions, are often described as 0-peak (p_{pk}) or peak-to-peak (p_{pk-pk}) sound pressures; however, these metrics do not account for different pulse shapes and durations. The sound pressure exposure, with units Pa^2 s, accounts for the shape of the pulse and provides a useful comparable metric for transient signals by integrating the squared-pressure of the pulse waveform time series over a time window,

$$E = \int_0^T p^2(t)dt.$$ (2)

Another useful and comparable metric for transient signals is the positive acoustic impulse, or pressure impulse, with units Pa s. The positive impulse is often used for studies on the effects of explosions on animals (Richardson *et al.*, 1995) and is the integral of pressure over the duration of the pulse,

$$J_p = \int_0^T p(t)dt.$$ (3)

Peak and rms sound pressures are often presented as levels in dB. To convert peak and rms pressures to levels, 20 times

the base-10 logarithm of the pressures was used such that L = 20 log$_{10}$(P/P$_0$), where P_0 = 1 μPa was the reference value of sound pressure, and L = sound pressure level (SPL) or the peak sound pressure level (L$_{pk}$) when P was p_{rms} or p_{pk}, respectively. Similarly, for the sound pressure exposure, the sound exposure level (SEL) was calculated as $SEL = 10\log_{10}(E/E_0)$, where the reference value was $E_0 = 1$ μPa^2 s. All metric terminology, units, and reference values were presented as per the International Organization for Standardization document for underwater acoustics (ISO 18405:2017, 2017).

E. Source level estimation

Source level is rarely measured in the field directly as it is referenced at 1 m range, which can be prohibitively close to the source, introducing complexities associated with the near field acoustic environment. Instead, SPLs were measured at ranges much greater than 1 m and range-dependent corrections for acoustic propagation loss, PL (reference value 1 m^2), were applied to estimate SLs at 1 m (reference value 1 μPa m) via the sonar equation,

$$SL = SPL + PL,$$ (4)

where values were in dB units (Urick, 1983). Similar to PL, but between two specified locations, neither of which was the source, was transmission loss (TL), expressed in dB and often a linear function of the base-10 logarithm of the range between the two locations such that

$$TL = X \log_{10}(R_2/R_1),$$ (5)

where R$_{1,2}$ were the ranges in meters from the source to locations 1 and 2, and X was the regression coefficient, or slope, of a linear regression model of SPL versus log$_{10}$(R).

Estimating SLs from acoustic waves that propagate along straight paths is typically much less complicated than from raypaths with additional energy loss from refraction, reflection, and absorption. For example, the sound pressure loss in a homogeneous, unbounded, and non-absorptive medium from a source radiating outward equally in all directions is termed spherical spreading, and X = 20 in Eq. (5) for short ranges and low frequencies (e.g., Urick, 1983). When the medium is bounded by top and bottom parallel planes, sound is reflected off of the planes and spreads cylindrically, propagating in a waveguide, resulting in a lower loss with X = 10; however, additional losses at the bounding planes can occur due to surface roughness scattering, waveform destructive interference, and, in the case of the seafloor boundary, refraction into substructure. Water column refraction can increase or decrease losses via focusing or defocusing sound waves as they bend toward or away from a receiver in a non-homogeneous medium. These complexities in losses arising from environmental factors need to be considered when estimating how SPL varies with distance from a source, for instance, when evaluating source impact on marine mammals.

F. Sound speed profile

The speed of sound in the ocean typically varies with depth, which affects how sound travels from source to receiver, including causing sound raypath refraction (i.e., bending) and creating shadow zone regions where direct raypaths are attenuated. Sound speed is a function of salinity, temperature, and pressure, with the latter two parameters having the largest effect through the water column. Temperature and pressure were measured and recorded using a Seabird (Bellevue, WA) SBE-39 attached to the line between the data logger pressure housing and the hydrophone (Fig. 3). This configuration provided two casts per deployment day, one down when the recorder was deployed and one up when the recorder was recovered. The three days of recording provided six casts, which were averaged to provide an overall mean temperature profile for the experiment. This temperature profile was used to estimate the mean sound speed profile using the Chen and Millero (1977) equations with a constant 35 ‰ salinity.

The sound speed profile was used to evaluate how raypaths travel between source and receiver in the area of the experiment. To estimate raypaths from source to receiver, we used BELLHOP, a ray tracing model software program run in MATLAB (Porter, 2011), along with the mean sound speed profile.

III. RESULTS

Over three experimental days, 648 seal bombs were deployed; 46 were logged as unexploded, and 542 were detected with the automatic detector (Table II). Unexploded seal bombs may not have been lit properly or had some other fault with the fuse or explosive. Seal bombs that were not detected either did not explode or likely had received sound pressures lower than the detector threshold due to sound propagation limitations such as long range or very shallow explosion depths (i.e., near the sea surface pressure release boundary).

A. Example single nearby shot

Seal bomb shots near the hydrophone receiver provided the highest received levels and best signal-to-noise ratio (SNR) for evaluating the arriving pulses. A shot from the closest-point-of-approach (CPA), where the explosion was nearly directly above the hydrophone on 2 June 2017, clearly shows four distinct pulses within the first 75 ms (Fig. 4). The direct arrival from the shot, ~262 m from the hydrophone, was a fast rising and slower decaying pulse, which was then reflected off the sea surface, causing a phase
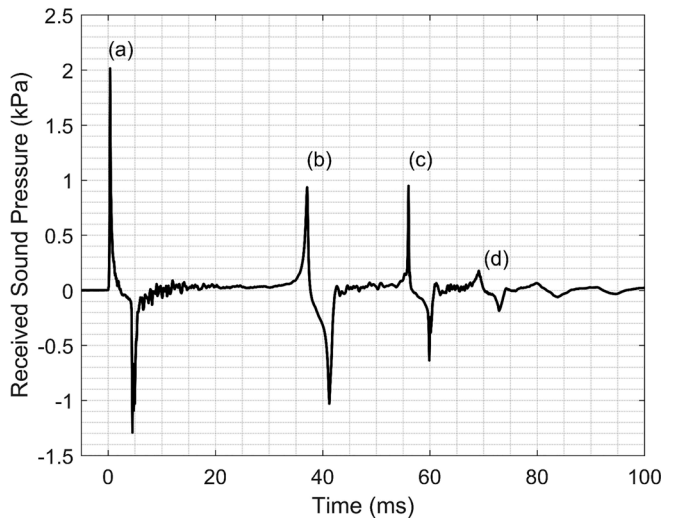

FIG. 4. Received sound pressure waveform for close range (262 m) seal bomb shot. (a) Initial pressure wave (0 ms) and its SSR (4 ms). (b) First bubble pulse (37 ms) and its SSR (41 ms); (c) second bubble pulse (56 ms) and its SSR (60 ms); (d) third bubble pulse (69 ms) and its SSR (73 ms). All SSR occurred ~4 ms after preceding arrivals, indicating the explosion depth was 3 m using 1500 m s^{-1} sound speed.

reversal and resulting negative pulse [Fig. 4(a)]. At about 37 ms after the first arrival, the first bubble pulse peaked, but with a slower rise time than the direct pulse, which was also reflected off the sea surface [Fig. 4(b)]. The third positive and negative pulses at ~56 ms were from the second bubble pulse and had the same initial steep character and phase as the first pulse and its sea surface reflection (SSR) [Fig. 4(c)]. The third bubble pulse and its SSR arrived ~69 ms after the direct pulse and at lower amplitude than the first two bubble pulses. All SSRs were around 4 ms after preceding positive pulses, indicating an approximate shot depth of 3 m using a 1500 m s^{-1} sound speed. The time difference between the positive pulse and its SSR for the third bubble pulse was ~0.25 ms less than for the first bubble pulse, indicating the third bubble pulse was shallower than the first. In general, with all recorded shots, the time between the direct first pulse arrival and the bubble pulses varied by a few milliseconds, showing slight variability in shot depth.

A more detailed evaluation of the first 2 ms from the CPA seal bomb shot (Fig. 5) showed the unfiltered (dotted) waveform had a leading transient with positive and negative pulses 30 μs apart, which we attributed to the hydrophone electronics. These transients only occurred on the direct and the second bubble pulses, likely due to their higher frequency content than the first and third bubble pulses, and were most prominent for close shots, decreasing with range. The LPF waveform showed a reduction in high frequencies and the leading transient but retained the pulse shape and area underneath the curve (i.e., pressure impulse, J_p), allowing various metrics to be calculated (Table III).

B. Peak sound pressure levels versus range

To examine our study area propagation environment, measured peak sound pressure levels from seal bomb shots

TABLE II. Seal bomb experiment days, deployed, unexploded, and detected.

Experiment day	01	02	03	Total
Date	30 May 2017	01 Jun 2017	02 Jun 2017	3 days
Deployed seal bombs	144	288	216	648
Unexploded seal bombs	18	19	9	46
Detected seal bombs	91	245	206	542

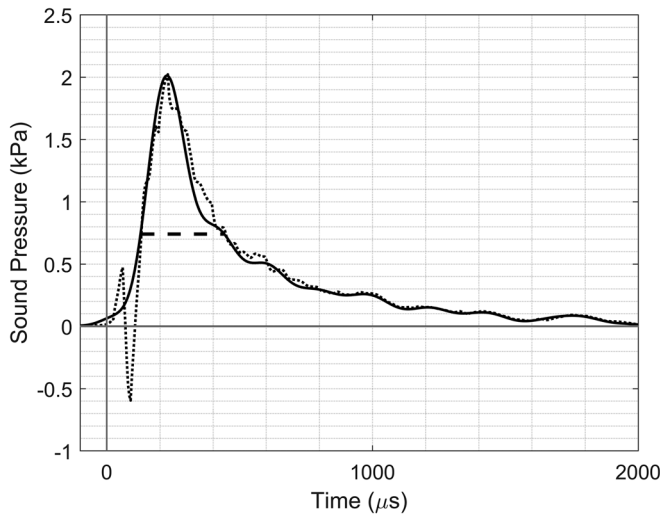J. Acoust. Soc. Am. **150** (3), September 2021

Wiggins *et al.* 1825

FIG. 5. Sound pressure waveform from recorded seal bomb explosion at CPA. Seal bomb with 2.33 g of flash powder was exploded at 262 m range from the hydrophone receiver. Dotted line, the unfiltered pulse with electronic noise; solid line, the filtered pulse using an eighth order Chebyshev type 2 LPF with a stop band edge at 10 kHz to minimize hydrophone electronic noise induced leading transient with positive and negative pulses.
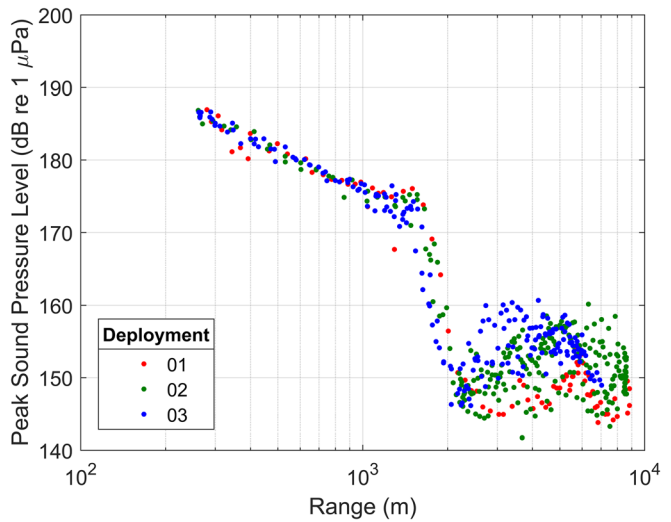

FIG. 6. (Color online) Seal bomb shot peak sound pressure levels versus logarithm base-10 ranges. Three distinct propagation regions: low-loss (260–1200 m), high-loss (1500–2000 m), and variable-loss (2000–9000 m). Dot colors represented deployment number. Linear regression models for the low-loss region showed spherical spreading ($X = 20$) between 260 and 340 m and were less lossy ($X = 19, 17$) between 400 and 800 m and between 800 and 1200 m, respectively.

were plotted against their ranges using a base-10 logarithm scale (Fig. 6). Three distinct regions grouped by ranges were apparent: low-loss (260–1200 m), high-loss (1500–2000 m), and variable-loss (2000–9000 m).

A linear regression model for peak sound pressure levels versus $\log_{10}(R)$ for the low-loss, short-range region provided a slope, or regression coefficient, $X = 18$, which was slightly less lossy than spherical spreading. Closer inspection of this region showed three sub-regions (260–340, 400–800, and 800–1200 m), each with slightly different and decreasing slopes of approximately 20, 19, and 17, respectively, becoming less lossy with increased range due to refraction focusing and eventually creating caustic-like effects ~1200–1500 m. When the recorded pulse waveforms from the low-loss region were scaled by their range and regression coefficient (i.e., $R^{X/20}$), they were all nearly identical for the first 500 µs of the pulse, showing low variability in shot pressure signatures at close ranges.

Refraction was the cause of high losses in the region between 1500 and 2000 m, with defocusing creating a TL

TABLE III. Seal bomb received peak sound pressure level, SPLs, pressure impulse, and SEL with charge mass of 2.33 g at CPA (i.e., 262 m range) over the frequency band 10 Hz–10 kHz.

Metric	Value	Time window (ms)
0-peak sound pressure levels	186 dB re 1 µPa	—
$SPL_{-3\,dB}$	185 dB re 1 µPa	0.120
$SPL_{-10\,dB}$	182 dB re 1 µPa	0.350
$SPL_{90\%}$	178 dB re 1 µPa	1.095
Pressure impulse	0.737 Pa s	2.00
SEL (primary pulse only)	149 dB re 1 µPa^2 s	2.00
SEL (primary + bubbles + reflections)	155 dB re 1 µPa^2 s	100

slope of $X \approx 130$ in a region where direct raypaths were strongly attenuated. Greater than 2000 m range, the raypath arrivals were complicated by sound waves reflecting off the seafloor and sea surface, in some cases multiple times, and there was no clear range-dependency of TL, showing more than 10 dB of peak sound pressure level variability (Fig. 6).

C. Refraction

To better understand the slight decrease in TL as range increases from the CPA and then the large increase in loss around 1500–2000 m range shown in Fig. 6, two-dimensional ray tracing in a depth-dependent sound speed model was performed and showed the effects of refraction. The sound speed profile for the model was estimated from an average of six depth-temperature casts during the experiment (Fig. 7).

The profile showed a large decrease in sound speed in the first ~20 m of depth, resulting in a large sound speed gradient near the sea surface. The amount of raypath curvature (i.e., refraction) is directly related to the magnitude of the sound speed gradient, with raypaths bending more in higher-gradient environments and when traveling more perpendicular to the direction of the gradient. For example, a raypath initially traveling horizontally (perpendicular to the direction of the sound speed gradient) in the upper 10 m of this model curved downward away from the sea surface such that a receiver at the same depth as the source received levels less than spherical spreading (i.e., defocusing) and a receiver at a deeper depth received levels greater than spherical spreading (i.e., focusing) for sufficiently close ranges.

A graphical example of this refraction effect showed raypaths traced from a 3 m deep shot with angles relative to the sea surface from $-3°$ to $45°$ in $2°$ increments for two
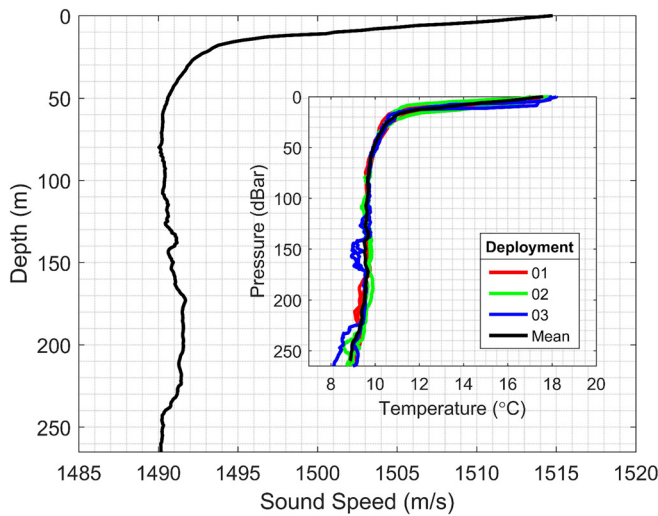
FIG. 7. (Color online) Sound speed and temperature profiles for study area. Sound speed profile was estimated based on the method of Chen and Millero (1977) using the mean (black line) temperature profile (inset) from two casts from each deployment (red, green, blue) and salinity of 35‰.

sound speed profiles: the one measured during this experiment and a homogeneous 1500 m s^{-1} profile exhibiting spherical spreading. In the refraction model [Fig. 8(a)] at the receiver depth (blue horizontal line), the area focusing raypaths was shown at ranges greater than ~1200 m up until the last ray (shot toward the sea surface) ~1700 m range. Beyond 1700 m, a shadow zone resulted, an area void of raypaths with very high TLs. The homogeneous sound speed model produced straight rays and no acoustic shadowing or focusing [Fig. 8(b)].
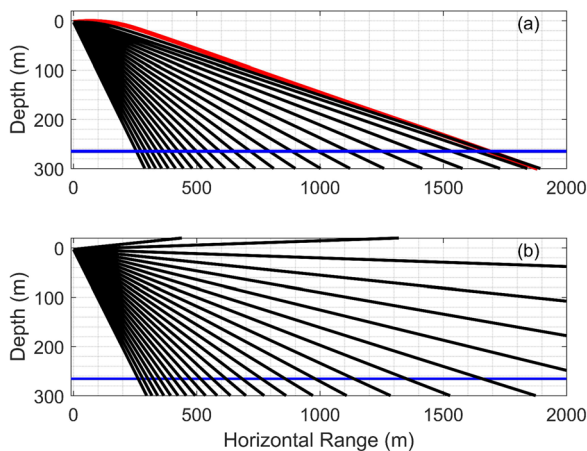

FIG. 8. (Color online) Raypaths traced in two models with different sound speed profiles. Rays were shot from a depth of 3 m in 2° increments from −3° to 45° relative to the sea surface. The blue horizontal line represents the hydrophone receiver at 265 m depth. (a) Sound speed profile from Fig. 7 with a strong gradient near the sea surface created strong refraction with rays becoming closer together as the range increased until the maximum range was reached (red raypath was shot toward the surface at −3° but refracted downward). (b) Homogeneous sound speed throughout the model caused all raypaths to be straight and evenly spaced in angle without refraction-caused shadow or focusing zones. Note that depth and range were at different scales (~1:2).

D. Estimated source metrics

To estimate seal bomb SLs from the sonar equation [Eq. (4)], we used the SPL measurements from the CPA shot at 262 m (Table III) and a spherical spreading PL $(20 \log_{10}(262 \text{ m}) = 48 \text{ dB re } 1 \text{ m}^2)$. The resulting SL was 233 dB re 1 μPa m over a 0.120 ms time window (Table IV). Similarly, SEL and pressure impulse were measured over a 2 ms window at CPA (Table III) and spherical spreading PL was applied, resulting in a sound exposure source level of 197 dB re 1 μPa^2 m^2 s and pressure impulse estimated 1 m from the source (source pressure impulse) of 193 Pa m s. Using a longer time window to include the bubble pulses and the surface reflections (100 ms) in addition to the primary pulse increased the sound exposure source level by 6 dB to 203 dB re 1 μPa^2 m^2 s (Table IV).

We chose the CPA shot levels because it was the closest shot to the reference 1 m providing good SNR with the least amount of PL, its raypath was straight and direct without adverse refraction effects, and other shots near CPA were nearly identical to the CPA shot when scaled by range. Without closer range measurements and with water depths much greater than source/receiver propagation paths, spherical spreading was an appropriate propagation model for these low-frequency, omni-directional seal bomb sources (Urick, 1983). Further supporting spherical spreading in this region was the TL slope from CPA to ~340 m, measured to be $X = 20$ (Fig. 6).

IV. DISCUSSION AND CONCLUSIONS

To characterize seal bomb sound pressure signatures, we recorded calibrated underwater received levels of shots and found the environment (i.e., temperature profile) had a significant effect on sound propagation for sources near the sea surface due to raypath refraction or bending, highlighting the need for good PL models to properly estimate received levels from SLs. For example, in the acoustically refractive model with a source at 3 m depth [Fig. 8(a)], a receiver near the sea surface and at ~500 m range would not receive direct raypaths, only steep angle rays reflected off of the seafloor, and received levels would be less than predicted by spherical spreading. Conversely, the same receiver

TABLE IV. Peak source level, SLs, source pressure impulse, and sound exposure source level estimates over the frequency band 10 Hz–10 kHz from seal bomb with charge mass of 2.33 g.

Metric	Value	Time window (ms)
0-peak source level	234 dB re 1 μPa m	—
SL$_{-3\text{ dB}}$	233 dB re 1 μPa m	0.120
SL$_{-10\text{ dB}}$	230 dB re 1 μPa m	0.350
SL$_{90\%}$	226 dB re 1 μPa m	1.095
Source pressure impulse	193 Pa m s	2.00
Sound exposure source level (primary pulse only)	197 dB re 1 μPa^2 m^2 s	2.00
Sound exposure source level (primary + bubbles + reflections)	203 dB re 1 μPa^2 m^2 s	100

at ∼100 m range may receive sound at higher levels than predicted with spherical spreading because of raypath focusing, and waveforms would likely be complicated with constructive and destructive interference from SSRs due to low grazing angles both from source and to receiver at shallow depths.

While our seal bomb estimated SL was a high SL in the ocean (e.g., Hildebrand, 2009), it was possible that nonlinear propagation with higher losses than spherical spreading occurred for seal bomb explosions at shorter ranges than measured in our experiment if seal bomb flash powder fast deflagration was similar to high explosive detonations generating a shockwave. For example, for a similar size charge of high explosives, the generated pulse would propagate nonlinearly to about 60 m with an additional ∼5 dB loss, or a factor of ∼1.8, before becoming linear propagation (Cole, 1948; Arons, 1954; Chapman, 1985), suggesting the SL could be as high as 238 dB re 1 μPa m. However, without additional measurements from shorter ranges than present here, we were required to use a spherical spreading PL model to estimate SL from the closest shot's received SPL.

While little is known about damage to marine mammals from underwater explosions, seal bomb source (i.e., at 1 m range) pressure impulse was estimated in this study to be at levels previously shown to cause tissue injury to medium-size terrestrial mammals held underwater (Yelverton et al., 1973), and based on an open-water seal bomb explosion study, Myrick et al. (1990a) suggested seal bombs cause damage to dolphins and other marine mammals if exploded within 4 m range.

In addition to physical tissue damage from close explosions, impulsive sounds may cause TTS or PTS damage in marine mammal hearing (e.g., Finneran, 2015). The National Oceanic and Atmospheric Administration (NOAA) National Marine Fisheries Service (NMFS) estimated PTS threshold for unweighted peak sound pressure level for earless seals (phocid) was 218 dB re 1 μPa, that for eared seals (otariid) was 232 dB re 1 μPa, and those for cetaceans ranged from 202 to 230 dB re 1 μPa, with TTS estimated as 6 dB lower, or effectively at farther ranges than PTS (National Marine Fisheries Service, 2018). These thresholds are all at or lower than the levels estimated for seal bombs at short ranges. This suggests PTS and TTS may be occurring for animals near seal bombs used in fisheries that employ them to deter marine mammals from depredation and accidental bycatch.

Peak levels and SPL are often used to describe underwater signals; however, they are incomplete for characterizing impulsive signals such as explosions, because no information on pulse shape is provided. Pulse duration provides additional details on the amount of energy that was contained in the pulse and the rate at which it was released. Time-integrated metrics, such as pressure impulse and SEL, are more comparable for impulsive signals because they account for the total energy in the pulse, not just the sound pressure amplitude. Furthermore, the complete received waveform from a seal bomb, not just the first pulse, should

be considered when evaluating impact because of additional impulsive sounds present from explosion bubble pulses and reflections off the sea surface. The total energy received was higher when the complete 100 ms waveform was used with sound exposure source level that was 6 dB higher than just the first 2 ms pulse. Furthermore, since seal bombs are often used repeatedly during fishing operations (Meyer-Löbbecke et al., 2016), cumulative SEL over the full period of event activity should be used to estimate the total amount of sound energy emitted into the environment. Expanding one step further, to properly assess how SEL relates to auditory injury thresholds in marine mammals, filtering of the full period time series by animal auditory frequency weighting functions during cumulative SEL calculations should be conducted (Southall et al., 2019).

ACKNOWLEDGMENTS

Arons, A. B. (**1954**). "Underwater explosion shock wave parameters at large distances from the charge," J. Acoust. Soc. Am. **26**, 343–346.

Cassano, E. R., Myrick, A. C., Glick, C. B., Holland, R. C., and Lennert, C. E. (**1990**). "The use of seal bombs on dolphins in the Eastern tropical pacific yellowfin tuna purse-seine fishery," in Administrative Report LJ-90-09 (Southwest Fisheries Center, National Marine Fisheries Service, La Jolla, CA).

Chapman, N. R. (**1985**). "Measurement of the waveform parameters of shallow explosive charges," J. Acoust. Soc. Am. **78**, 672–681.

Chen, C.-T., and Millero, F. J. (**1977**). "Speed of sound in seawater at high pressures," J. Acoust. Soc. Am. **62**, 1129–1135.

Cole, R. H. (**1948**). Underwater Explosions (Princeton University, Princeton, NJ).

Finneran, J. J. (**2015**). "Noise-induced hearing loss in marine mammals: A review of temporary threshold shift studies from 1996 to 2015," J. Acoust. Soc. Am. **138**, 1702–1726.

Hildebrand, J. A. (**2009**). "Anthropogenic and natural sources of ambient noise in the ocean," Mar. Ecol. Prog. Ser. **395**, 5–20.

ISO 18405:2017 (**2017**). "Underwater acoustics—Terminology" (International Organization for Standardization, Geneva, Switzerland).

Madsen, P. T. (**2005**). "Marine mammals and noise: Problems with root mean square sound pressure levels for transients," J. Acoust. Soc. Am. **117**, 3952–3957.

Meyer-Löbbecke, A., Debich, A. J., Širović, A., Trickey, J. S., Roch, M. A., Carretta, J. V., Fraiser, K., Wiggins, S. M., Hildebrand, J. A., Denzinger, A., Schnitzler, H.-U., and Baumann-Pickering, S. (**2016**). "Noise from explosive deterrents used by California fisheries and possible effects on

11 January 2024 18:25:46

marine life (poster)," in *Proceedings of the 4th International Conference on the Effects of Noise on Aquatic Life*, July 10–16, Dublin, Ireland.

Myrick, A. C., Cassano, E. R., and Oliver, C. W. (**1990a**). "Potential for physical injury, other than hearing damage, to dolphins from seal bombs used in the yellowfin tuna purse-seine fishery: Results from open-water tests," in *Administrative Report LJ-90-07* (Southwest Fisheries Center, National Marine Fisheries Service, La Jolla, CA).

Myrick, A. C., Fink, M., and Glick, C. B. (**1990b**). "Identification, chemistry, and behavior of seal bombs used to control dolphins in the yellowfin tuna purse-seine fishery in the Eastern tropical pacific: Potential hazards," in *Administrative Report LJ-90-08* (Southwest Fisheries Center, National Marine Fisheries Service, La Jolla, CA).

National Marine Fisheries Service (**2018**). "2018 Revisions to: Technical Guidance for Assessing the Effects of Anthropogenic Sound on Marine Mammal Hearing (Version 2.0): Underwater Thresholds for Onset of Permanent and Temporary Threshold Shifts," NOAA Technical Memorandum NMFS-OPR-59 (National Oceanic and Atmospheric Administration, Washington, DC).

Porter, M. B. (**2011**). *The BELLHOP Manual and User's Guide: Preliminary Draft* (Heat, Light, and Sound Research, Inc., La Jolla, CA).

Richardson, W. J., Greene, C. R., Malme, C. I., and Thomson, D. H. (**1995**). *Marine Mammals and Noise* (Academic, San Diego, CA).

Southall, B. L., Bowles, A. E., Ellison, W. T., Finneran, J. J., Gentry, R. L., Greene, C. R., Kastak, D., Ketten, D. R., Miller, J. H., Nachtigall, P. E., Richardson, W. J., Thomas, J. A., and Tyack, P. L. (**2007**). "Criteria for Behavioral Disturbance," Aquat. Mamm. **33**, 446–473.

Southall, B. L., Finneran, J. J., Reichmuth, C., Nachtigall, P. E., Ketten, D. R., Bowles, A. E., Ellison, W. T., Nowacek, D. P., and Tyack, P. L. (**2019**). "Marine mammal noise exposure criteria: Updated scientific recommendations for residual hearing effects," Aquat. Mamm. **45**, 125–232.

Stonebraker, M. (**2018**). (personal communication).

Urick, R. J. (**1983**). *Principles of Underwater Sound* (McGraw-Hill, New York).

Weston, D. E. (**1960**). "Underwater explosions as acoustic sources," Proc. Phys. Soc. **76**, 233–249.

Wiggins, S. M., and Hildebrand, J. A. (**2007**). "High-frequency acoustic recording package (HARP) for broad-band, long-term marine mammal monitoring," in *Proceedings of the International Symposium on Underwater Technology 2007 and International Workshop on Scientific Use of Submarine Cables & Related Technologies 2007*, April 17–20, Tokyo, Japan, pp. 551-557.

Yelverton, J. T., Richmond, D. R., Fletcher, E. R., and Jones, R. K. (**1973**). "Safe distances from underwater explosions for mammals and birds," Report No. DNA 3114T (Defense Nuclear Agency, Washington, DC).

11 January 2024 18:25:46